Bioconjugate Chemistry

Article

pubs.acs.org/bc

Structure Binding Relationship of Galactosylated Glycoclusters toward *Pseudomonas aeruginosa* Lectin LecA Using a DNA-Based Carbohydrate Microarray

Béatrice Gerland,[†] Alice Goudot,[‡] Caroline Ligeour,[†] Gwladys Pourceau,[†] Albert Meyer,[†] Sébastien Vidal,[§] Thomas Gehin,[‡] Olivier Vidal,[∥] Eliane Souteyrand,[‡] Jean-Jacques Vasseur,[†] Yann Chevolot,*[,‡] and François Morvan*[,†]

[†]Institut des Biomolécules Max Mousseron (IBMM), UMR 5247 CNRS - Université Montpellier 1 - Université Montpellier 2, place Eugène Bataillon, CC1704, 34095 Montpellier cedex 5, France

[‡]Institut des Nanotechnologies de Lyon (INL), UMR 5270 CNRS Ecole Centrale de Lyon, 36 avenue Guy de Collongue, 69134 Ecully cedex, France

[§]Institut de Chimie et Biochimie Moléculaires et Supramoléculaires (ICBMS), Laboratoire de Chimie Organique 2 – Glycochimie, UMR 5246, CNRS, Université Claude Bernard Lyon 1, 43 Boulevard du 11 Novembre 1918, 69622 Villeurbanne, France

[∥]Unité de Glycobiologie Structurelle et Fonctionnelle (UGSF), UMR 8576 Université de Lille 1, Cité Scientifique Avenue Mendeleiev, Bat C9, 59655 Villeneuve d'Ascq cedex, France

Supporting Information

ABSTRACT: *Pseudomonas aeruginosa* (PA) is a major public health issue due to its impact on nosocomial infections as well as its impact on cystic fibrosis patient mortality. One of the main concerns is its ability to develop antibiotic resistance. Therefore, inhibition of PA virulence has been proposed as an alternative strategy to tackle PA based infections. LecA (or PA-IL), a galactose binding lectin from PA, is involved in its virulence. Herein, we aimed at designing high affinity synthetic ligands toward LecA for its inhibition and at understanding the key parameters governing the binding of multivalent galactosylated clusters. Twenty-five glycoclusters were synthesized and their bindings were studied on a carbohydrate microarray. Monosaccharide centered clusters and linear comb-like clusters were synthesized with different linkers separating the core and the galactosyl residues. Their length, flexibility, and aromaticity were varied. Our results showed that the binding profile of LecA to galactosylated clusters was dependent on both the core and the linker and also that the optimal linker was different for each core. Nevertheless, an aryl group in the linker structure drastically improved the binding to LecA. Our results also suggest that optimal distances are preferred between the core and the aromatic group and the core and the galactose.

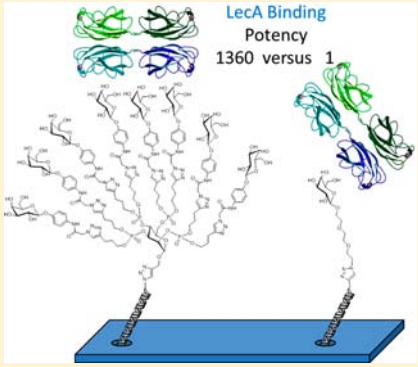

INTRODUCTION

Pseudomonas aeruginosa (PA) is a Gram-negative, aerobic, and clinically important opportunistic pathogen often related to hospital infections, as it is responsible for 10−30% of hospital-acquired infections.[1] It is also the most frequent pathogen, progressively leading to chronic inflammation and to the degradation of the respiratory tract of Cystic Fibrosis patients.[2] Consequently, regarding the emergence of resistance of most pathogenic bacteria, especially PA, to antibiotics, the development of new antibacterial agents able to escape the mechanisms of resistance or of new modes of action has become imperative and is a major research challenge to treat or prevent infectious diseases. Along this line, synthetic clusters able to compete with the natural ligands of lectins can potentially prevent PA infection and could be an ideal alternative to antibiotic treatments.[3−5] PA takes advantage of a large arsenal of virulence factors to adapt and proliferate in human airways. Among them, *Pseudomonas aeruginosa* PA-IL (LecA) a soluble lectin binding D-galactose and its derivatives[6] are of particular interest. PA-IL acts as an adhesion factor promoting colonization of the lung epithelium,[7] as well as acting as a bacterial aggregation prerequisite to the biofilm establishment.[8] The lectin also displays a cytotoxic effect toward host epithelium either directly as has been shown in human respiratory cells in vitro[9] or indirectly by inducing a permeability defect on intestinal epithelium to another cytotoxic exoproduct, exotoxin A.[10]

The ability to inhibit such virulent factors as *Pseudomonas aeruginosa* lectin A (LecA or PA-IL) offers the perspective of a new approach for antibacterial therapies in which the bacterial

Received: November 15, 2013
Revised: January 20, 2014
Published: January 21, 2014

dx.doi.org/10.1021/bc4005365 | *Bioconjugate Chem.* 2014, 25, 379−392

functions contributing to the infection are targeted. LecA is a tetravalent lectin with a nearly rectangular shape with binding sites a distance of 71 Å on the long side and 32 Å on the short side.[11,12] The binding of LecA for monovalent galactosides is in the micromolar range and is influenced by the structure of the aglycon with enhanced binding for phenyl-β-Gal. Indeed, the introduction of a β-anomeric phenyl aglycon creates additional hydrophobic interactions.[6,13] The binding of LecA can reach the nanomolar range when taking advantage of the so-called cluster effect.[14−16] In this case, multivalent carbohydrate ligands are designed and the binding per carbohydrate residues to the target lectin can be enhanced compared to the monovalent ligand.[3−5] Several galactosylated glycoclusters have been reported and their binding to LecA discussed.[3,4,17−19] The extent of the enhancement is, among other things, a function of the topology, as the residues should fit in the multiple sites of the lectins.

The topology of a glycomimetic is an important factor for its efficient binding to a lectin. It is a combination of not only the scaffold but also the linker structure between the terminal carbohydrate epitopes and the scaffold. Furthermore, the nature of the linker could provide additional interactions (e.g., hydrogen bond, $\pi-\pi$ stacking, hydrophobic interactions, ionic bonds)[20] with the amino acids near the carbohydrate recognition domain (CRD) of the targeted lectin allowing an increase of the binding.

The flexibility and the length of the linker also play a key role. Ideally, the topology of the carbohydrate residues should match the binding sites of the lectin on an atomic scale for maximal interaction. However, since this is almost unachievable, some flexibility should be introduced through the linker and consequently lead to an entropic cost of the binding.

This trade-off is illustrated in a study by Pieters et al.[21] in which divalent galactosyl clusters bearing PEG spacers are less potent than more rigid clusters. However, as the rigidity increases, the length seems to become a critical parameter. In another study, Cecioni et al.[18] have underlined the importance of the linker design in calixarene-based galactose constructs. Too-rigid linkers prevented the four galactosyl residues from interacting simultaneously with the four binding sites of the lectin, leading to increased stoichiometry. Furthermore, they showed that increasing the length of the linker from diethylene glycol linker to triethylene glycol did not significantly influence the binding. This is probably due to the low rigidity of PEG based linker and is in agreement with the findings of Pieters et al.[21]

Herein aiming at designing high affinity multivalent clusters targeting LecA, the influence of the linker in combination with different scaffolds was studied.[22] The linker length, the rigidity, and the position of the aromatic aglycon were varied and their binding to LecA was studied on DNA-Directed Immobilized Glycocluster array.[20,23]

EXPERIMENTAL PROCEDURES

The syntheses of phosphoramidites **1**,[24] **2**,[25,26] **1a**,[27] **1b**[27], and **1c**[28] and azide solid support **5**[29] were previously reported. Carbohydrate derivatives **3**,[30] **4a**,[31] **4b**,[32] **4c**,[33] **4d**,[18] **4e**,[32] **6**,[30] propagyl galactopyranoside, and propargyl glucopyranoside[34] were prepared according to literature procedures.

***N*^{1}-(2′,3′,4′,6′-Tetra-*O*-acetyl-β-D-galactopyranosyl)-thymine 15.** *N*,*O*-Bis(trimethylsilyl) acetamide (BSA) (1.5 mL, 6.1 mmol) was added to a suspension of thymine (327 mg, 2.6 mmol) and 1,2,3,4,6-penta-*O*-acetyl-D-galactopyranose (1.09 g, 2.56 mmol) in dichloroethane (25 mL). The mixture was stirred under argon at room temperature for 20 min. After addition of TMSOTf (2.2 mL, 12.1 mmol) the reaction mixture was heated under reflux for 2 h 30 min. The resultant mixture was cooled to room temperature and the solvents were evaporated in vacuum. The resulting oil was diluted in ethyl acetate (100 mL) and washed with an aqueous saturated solution of $NaHCO_3$ (100 mL) and brine (2 × 100 mL). After drying with Na_2SO_4, filtration, and concentration, the resultant oil was purified by silica gel column chromatography (EtOAc/cyclohexane, 8:2, v/v) to afford the desired compound **20** (782 mg, 67%) as a white foam. ^{1}H NMR (300 MHz, $CDCl_3$) δ 8.80 (s, 1H, NH), 7.16 (d, J = 1.2 Hz, 1H, H-6), 5.84 (d, J = 9.1 Hz, 1H, H-1′), 5.51 (d, J = 3.2 Hz, 1H, H-2′), 5.31 (t, J = 9.6 Hz, 1H, H-3′), 5.21 (dd, J = 10.2 Hz, J = 3.3 Hz, 1H, H-5′), 4.18−4.14 (m, 3H, H-4′, H-6′), 2.06−2.00 (m, 12H, OAc), 1.98 (d, J = 1.2 Hz, 3H, CH_3). ^{13}C NMR (75 MHz, $CDCl_3$) δ 170.4−169.7 (4s, CO), 163.1 (C-4), 150.4 (C-2), 134.8 (C-6), 112.1 (C-5), 80.6 (C-1′), 73.8 (C-5′), 70.9 (C-3′), 67.1, 67.0 (C-2′, C-4′), 61.3 (C-6′), 21.0, 20.7, 20.5 (3s, $COCH_3$), 12.6 (CH_3). HR-ESI-QToF MS (positive mode): m/z calcd for $C_{19}H_{25}N_2O_{11}$ $[M+H]^+$: 457.1457 found 457.1458.

***N*^{1}-(2′,3′,4′,6′-Tetra-*O*-acetyl-β-D-galactopyranosyl)-3-(4-bromobutyl)thymine 16.** A solution of *N*^{1}-(2′,3′,4′,6′-tetra-*O*-acetyl-β-D-galactopyranosyl)-thymine **15** (350 mg, 0.77 mmol) in anhydrous dimethylformamide (4 mL) was stirred for 5 min with potassium carbonate (318 mg, 2.30 mmol). Then, 1,4-dibromobutane (919 μL, 7.70 mmol) was added and the mixture was refluxed for 4 h and heated at 70 °C overnight. The reaction mixture was then concentrated to give an oil, which was diluted in dichloromethane (20 mL) and washed with an aqueous saturated solution of $NaHCO_3$ (20 mL) and brine (2 × 20 mL). The organic layer was dried (Na_2SO_4), filtered, and concentrated. The crude product was purified by silica gel column chromatography (EtOAc/cyclohexane, 4:6, v/v) to afford the desired compound **16** (270 mg, 59%) as a pale yellow foam. ^{1}H NMR (300 MHz, $CDCl_3$) δ 7.14 (d, J = 1.3 Hz, 1H, H-6), 5.89 (d, J = 9.0 Hz, 1H, H-1′), 5.51 (d, J = 3.0 Hz, 1H, H-5′), 5.30 (t, J = 9.5 Hz, 1H, H-2′), 5.21 (dd, J = 10.2 Hz, J = 3.3 Hz, 1H, H-3′), 4.21−4.09 (m, 3H, H-4′, H-6′), 3.97 (t, J = 7.1 Hz, 2H, NCH_2), 3.44 (t, J = 6.5 Hz, 2H, CH_2Br), 2.23 (s, 3H, CH_3), 2.06 (s, 3H, $COCH_3$), 2.00 (2s, 9H, $COCH_3$), 1.90 (m, 2H, CH_2CH_2Br), 1.78 (m, 2H, NCH_2CH_2). ^{13}C NMR (75 MHz, $CDCl_3$) δ 170.4−169.4 (4s, CO), 162.8 (C-4), 151.1 (C-2), 132.7 (C-6), 111.4 (C-5), 81.0 (C-1′), 73.7 (C-5′), 70.9 (C-3′), 67.3, 66.9 (C-2′, C-4′), 61.7 (C-6′), 40.6 (NCH_2), 33.0 (CH_2Br), 30.0, 26.4 (NCH_2CH_2, $CH_2CH_2N_3$), 20.7, 20.5, 20.4 (3s, $COCH_3$), 13.3 (CH_3). HR-ESI-QToF MS (positive mode): m/z calcd for $C_{23}H_{32}N_2O_{11}$Br $[M+H]^+$: 591.1177, found 591.1189.

***N*^{1}-(2′,3′,4′,6′-Tetra-*O*-acetyl-β-D-galactopyranosyl)-3-(4-azidobutyl)thymine 4f.** A solution of **16** (231 mg, 0.39 mmol) in anhydrous dimethylformamide (3 mL) was stirred at 100 °C for 24 h with sodium azide (203 mg, 3.12 mmol). After addition of dichloromethane (10 mL), the reaction was washed with brine (3 × 20 mL). The organic layer was dried (Na_2SO_4), filtered, and concentrated to afford the desired product **4f** (214 mg, 99%) as a colorless oil. ^{1}H NMR (400 MHz, $CDCl_3$) δ 7.10 (d, J = 1.3 Hz, 1H, H-6), 5.86 (d, J = 8.9 Hz, 1H, H-1′), 5.46 (dd, J = 3.1 Hz, J = 0.8 Hz, 1H, H-5′), 5.24 (t, J = 9.4 Hz, 1H, H-2′), 5.19 (dd, J = 10.1 Hz, J = 3.2 Hz, 1H, H-3′), 4.16−4.12 (m, 2H, H-4′, H-6′), 4.06 (dd, J = 8.8 Hz, J = 12.8 Hz, 1H, H-6′), 3.91 (t, J = 7.1 Hz, 2H, NCH_2), 3.27 (t, J = 6.7 Hz, 2H,

dx.doi.org/10.1021/bc4005365 | Bioconjugate Chem. 2014, 25, 379−392

CH_2N_3), 2.17 (s, 3H, CH_3), 2.00 (s, 3H, $COCH_3$), 1.94 (2s, 9H, $COCH_3$), 1.67−1.62 (m, 2H, NCH_2CH_2), 1.60−1.54 (m, 2H, $CH_2CH_2N_3$). ^{13}C NMR (100 MHz, $CDCl_3$) δ 170.3−169.6 (4s, CO), 162.8 (C-4), 151.0 (C-2), 132.9 (C-6), 111.3 (C-5), 81.2 (C-1′), 73.6 (C-5′), 70.9 (C-3′), 67.4, 67.0 (C-2′, C-4′), 61.3 (C-6′), 51.0 (CH_2N_3), 40.8 (NCH_2), 26.2, 24.8 (NCH_2CH_2, $CH_2CH_2N_3$), 20.6, 20.4, 20.3 (3s, $COCH_3$), 13.3 (CH_3). HR-ESI-QToF MS (positive mode): m/z calcd for $C_{23}H_{32}N_5O_{11}$ $[M+H]^+$: 554.2081, found 554.2098.

Immobilization on Azide Solid Support 5 of Propargyl Hexopyranosides by Cu(I)-Catalyzed Alkyne Azide 1,3-Dipolar Cycloaddition. An aqueous solution of propargyl hexopyranoside (α-mannopyranoside **6**, β-galactopyranoside, or β-glucopyranoside) (100 mM, 175 μL), freshly prepared aqueous solutions of $CuSO_4$ (100 mM, 14 μL) and sodium ascorbate (500 mM, 14 μL), water (147 μL), and MeOH (350 μL) were added to 3.5 μmol of azide solid support **5**. The resulting mixture was treated in a sealed tube with a microwave synthesizer at 60 °C for 45 min (premixing time: 30 s). The temperature was monitored with an internal infrared probe. The solution was removed, and CPG beads were washed with H_2O (3 × 2 mL), MeOH (3 × 2 mL), and CH_3CN (3 × 2 mL), and dried affording solid-supported hexose.

General Procedure for Introduction of Alkynyl or Bromohexyl Phosphoramidites on Hexose Hydroxyls. Solid-supported hexose derivatives (1 μmol scale) were treated by phosphoramidite chemistry, on a DNA synthesizer, with alkynyl phosphoramidites **1**, **1a**−**c**, or 6-bromohexyl phosphoramidite **2**. Only coupling and oxidation steps were performed. For the coupling step, benzylmercaptotetrazole was used as activator (0.3 M in anhydrous CH_3CN) and phosphoramidite **1**, **2**, or **1a**−**c** (0.2 M in anhydrous CH_3CN) was introduced three times (120 μmol) with a 180 s coupling time. Oxidation was performed with commercial solution of iodide (0.1 M I_2, THF/pyridine/water 90:5:5) for 15 s.

General Procedure for Azidation. The solid-supported oligonucleotides bearing the tetrabromohexyl hexoses (1 μmol) were treated with a solution of tetramethylguanidine azide ($TMG-N_3$) (31.6 mg, 200 equiv) and NaI (30 mg, 200 equiv) in DMF (1 mL) for 1 h at 65 °C. The beads were washed with DMF (3 × 2 mL), H_2O (3 × 2 mL), and CH_3CN (3 × 2 mL), and then dried by flushing with argon.

General Procedure for Elongation of DNA Sequences and Labeling with Cy3. The DNA sequences were synthesized on the solid-supported scaffolds at the 1 μmol scale on a DNA synthesizer (ABI 394) by standard phosphoramidite chemistry. For the coupling step, benzylmercaptotetrazole was used as activator (0.3 M in anhydrous CH_3CN), commercially available nucleosides phosphoramidites (0.09 M in anhydrous CH_3CN) were introduced with a 20 s coupling time and Cy3 amidite (0.06 M in anhydrous CH_3CN) with a 180 s coupling time. The capping step was performed with acetic anhydride using commercial solution (Cap A: Ac_2O/pyridine/THF, 10:10:80 and Cap B: 10% *N*-methylimidazole in THF) for 15 s. Each oxidation was performed for 15 s. Detritylation was performed with 2.5% DCA in CH_2Cl_2 for 35 s.

General Procedure for Deprotection of Solid-Supported Oligonucleotides. The CPG beads bearing modified oligonucleotides were transferred to a 4 mL screw top vial and treated with 2 mL of concentrated aqueous ammonia for 15 h at room temperature and warmed to 55 °C for 2 h. For each compound, the supernatants were withdrawn and evaporated to dryness. Residues were dissolved in water.

General Procedure for the Elongation by Hydrogenophosphonate Chemistry. Elongation was performed on a DNA synthesizer (ABI 394) using an *H*-phosphonate chemistry cycle starting from a 1,3-propanediol solid support (1 μmol). The detritylation step was performed with 2.5% DCA in CH_2Cl_2 for 35 s. Then, dimethanolcyclohexane (DMCH) *H*-phosphonate monoester **9**[35] or commercially available thymidine *H*-phosphonate monoester (0.06 M in anhydrous CH_3CN/C_5H_5N 1:1 v/v) and pivaloyl chloride as activator (200 mM in anhydrous CH_3CN/C_5H_5N 1:1 v/v) were passed 6 times through the column alternatively for 5 s (30 molar excess). The cycle was repeated as required to afford the desired scaffolds with 2 to 5 DMCH motifs or 4 dT motifs.

General Procedure for Amidative Oxidation. The solid-supported *H*-phosphonate diester scaffolds (1 μmol) were treated back and forth using two syringes, with 2 mL of a solution of 10% of propargylamine in CCl_4/C_5H_5N (1:1 v/v) for 30 min. The CPG beads were washed with C_5H_5N (2 × 2 mL) and CH_3CN (3 × 2 mL) and then dried by flushing with argon. Then the elongation of the oligonucleotides and labeling with Cy3 were performed by phosphoramidite chemistry as described above.

*General Procedure for CuAAC Reaction. Procedure for Introduction of Azido-Functionalized D-Galactose Derivatives **4a**−**f**.* To a solution of 5′-fluorescent-3′-alkyne oligonucleotide (100 nmol in 100 μL of H_2O) were added azido-functionalized galactoses **4a**−**f** (3 equiv per alkyne function, 100 mM in MeOH), 1 mg of Cu(0) nanopowder, triethylammonium acetate buffer 0.1 M, pH 7.7 (25 μL), water, and MeOH to obtain a final volume of 250 μL (water MeOH, 1:1, v/v). The tube containing the resulting preparation was sealed and placed in a microwave synthesizer initiator from Biotage with a 30 s premixing time at 60 °C for 60 min.

*Procedure for Introduction of Propargyl β-D-Galactopyranoside **3**.* To a solution of 5′-fluorescent-3′-hexose-centered tetra azidohexyl oligonucleotide (100 nmol in 100 μL of H_2O) were added propargyl 2,3,4-tri-*O*-acetyl-β-D-galactopyranoside **3** (5 equiv per azide function, 100 mM in MeOH), 1 mg of Cu(0) nanopowder, triethylammonium acetate buffer 0.1 M, pH 7.7 (25 μL), water, and MeOH to obtain a final volume of 250 μL (water MeOH, 1:1, v/v). The tube containing the resulting preparation was sealed and placed in an oil bath with magnetic stirring at 60 °C for 60 min.

Workup of CuAAC Reactions and HPLC Purifications. EDTA (400 μL) was added to the mixtures, and after centrifugation, the supernatants were withdrawn to eliminate Cu(0) and were desalted by size-exclusion chromatography on NAP10. After evaporation, the 5′-fluorescent 3′-(acetylated-glycomimetic) oligonucleotides were dissolved in water and purified by reversed-phase preparative HPLC. Pure compounds were treated with concentrated aqueous ammonia (3 mL) for 2 h at room temperature to remove acetyl groups, and evaporated to dryness (purity >97%). Final compounds were purified again by reversed-phase preparative HPLC using a linear gradient from 8% to 32% of acetonitrile in TEAAc buffer pH 7 over 20 min. Residues were dissolved in water for subsequent analyses.

Fabrication of DDI-Microarrays. Fabrication of Microstructured Slides. Microstructured slides are featured with 40 square wells (3 mm width, 60 ± 1 μm depth, with a 4.5 mm spacing between each microreactor). Microreactors were

dx.doi.org/10.1021/bc4005365 | *Bioconjugate Chem.* 2014, 25, 379−392

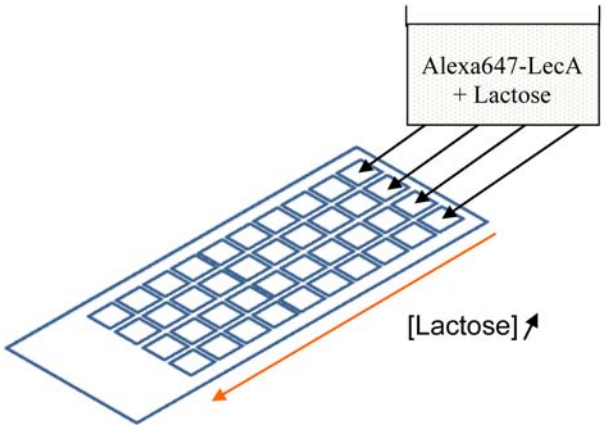

[Lactose]$_{final}$ (μM)
0
0.00001
0.0001
0.0005
0.001
0.005
0.01
0.05
0.1
1
5
10
50
100
500
1000
5000
10000
100000
300000

Figure 1. General sketch map of the miniaturized biosystem (microstructured glass slide) for IC_{50} determinations with a lactose concentration gradient.

fabricated by photolithography and wet etching process onto flat glass slides. These methods are detailed elsewhere.[36,37]

Silanization of the Glass Slides. According to the protocol developed by Dugas et al.,[38,39] slides were functionalized as follows: after piranha treatment, the slides were heated under dry nitrogen at 150 °C for 2 h. Next, dry pentane and *tert*-butyl-11-(dimethylamino)silylundecanoate were added at room temperature. After 2 h of incubation, the pentane was evaporated and the slides were heated at 150 °C overnight. Functionalized slides were obtained after washing in THF and rinsing in water. The ester function was converted into the corresponding acid using formic acid for 7 h at room temperature. Acid group bearing slides were activated for amine coupling with *N*-hydroxysuccinimide (0.1 M) and di(isopropyl)carbodiimide (0.1 M) in dry THF, overnight at room temperature. Finally, the slides were rinsed in THF and dichloromethane for 10 min under ultrasound.

Immobilization of Amino-Modified Oligonucleotides. Four amino modified oligonucleotides were purchased from Eurogentec. Spotting of 0.3 nL of the corresponding oligonucleotides at 25 μM in PBS_{10X} (pH 8.5) at the bottom of each reactor (64 spots per well) with the spotting robot: *Scienion sciFLEX ARRAYER s3*. The substitution reaction was performed overnight at room temperature in a water saturated atmosphere, and then, water was allowed slowly to evaporate. Washing of the slides was performed with $SDS_{0.1\%}$ at 70 °C for 30 min and deionized water briefly.

Blocking Step. To prevent nonspecific adsorption during the hybridization step, all slides were blocked with bovine serum albumin (BSA). Blocking was performed with BSA 4% solution in PBS_{1X} (pH 7.4), at 37 °C for 2 h. The washing steps were as follows: 3 × 3 min in PBS-Tween$_{0.05\%}$ followed by 3 × 3 min in PBS_{1X}, and finally the glasses were rinsed with deionized water before being dried by centrifugation.

Hybridization of Glycomimetics. Hybridization Step. 2 μL of a solution of each glycoconjugate bearing a DNA tag, at 1 μM in PBS_{1X} (pH 7.4), was placed at the bottom of the corresponding well and allowed to hybridize overnight at room temperature in a water vapor saturated chamber. The samples were washed in saline-sodium citrate 2× (SSC_{2X}), $SDS_{0.1\%}$ at 51 °C for 1 min, followed by SSC_{2X} at room temperature for an additional 5 min, and finally rinsed with deionized water before being dried by centrifugation.

Blocking Step. After hybridization, all slides were blocked again with bovine serum albumin (BSA). Blocking was performed with BSA 4% solution in PBS_{1X} (pH 7.4), at 37 °C for 1 h. The washing steps are as follows: 3 × 3 min in PBS-Tween$_{0.05\%}$ followed by 3 × 3 min in PBS_{1X}, and briefly rinsing with deionized water before being dried by centrifugation.

Lectin Labeling. Alexa647 Labeling of LecA Lectin. LecA was labeled with Alexa Fluor 647 Microscale Protein Labeling Kit (A30009) from Invitrogen. LecA was kindly provided by Dr. Anne Imberty (CERMAV, Grenoble). LecA cloning and production was done according to the protocol reported by Blanchard et al.[40] LecA can be purchased from Elicityl (www.elicityl-oligotech.com). In brief, 100 μL of a 1 mg/mL solution of LecA (MW: 51 kDa) diluted in PBS_{1X} (pH 7.4) was mixed with 10 μL of 1 M sodium bicarbonate (pH 8.3). The appropriate volume of reactive dye solution at 7.94 nmol/μL was transferred into the reaction tube containing the pH-adjusted protein. Reaction mixture was mixed for 15 min at room temperature before purification on a spin column (gel resin container) in order to separate the labeled protein from unreacted dye.

Lectin concentration and the dye to lectin ratio were estimated by optical density using a tray cell system combined to a *Safas Monaco UV mc*^{2} spectrophotometer reading the absorbance at 281 and 650 nm. LecA concentration was estimated to be 13.53 μM with a degree of labeling of 0.20 dyes for tetrameric LecA. Alexa647-LecA was aliquoted and stored at −20 °C. Aliquots were thawed gently at 4 °C just before use.

IC_{50} Determination with "On Chip" Biological Recognition. Preparation of the Solutions of Incubation. Lectin LecA (0.12 μM final concentration), BSA (2% final concentration), and $CaCl_2$ (1 μg/mL final concentration) was diluted in PBS_{1X} (pH 7.4). Into each microtube was added the inhibitor lactose at the desired final concentration (Figure 1).

Incubation of the Complex Glycoconjugate-Lectin on the Microreactors. Two microliters of each solution was deposited in the corresponding microwells and the slide was incubated at 37 °C in a water vapor saturated chamber for 3 h. The washing steps are as follows: PBS-Tween$_{0.02\%}$ 5 min at 4 °C, then briefly in deionized water, and drying by centrifugation.

Fluorescence Scanning. Slide was scanned at 532 nm, then at 635 nm with the Microarray scanner, GenePix 4100A software package (Axon Instruments; λ_{ex} 532/635 nm and λ_{em} 575/670 nm). The fluorescence signal of each conjugate was determined as the average of the mean fluorescence signal of 64 spots.

dx.doi.org/10.1021/bc4005365 | *Bioconjugate Chem.* 2014, 25, 379−392

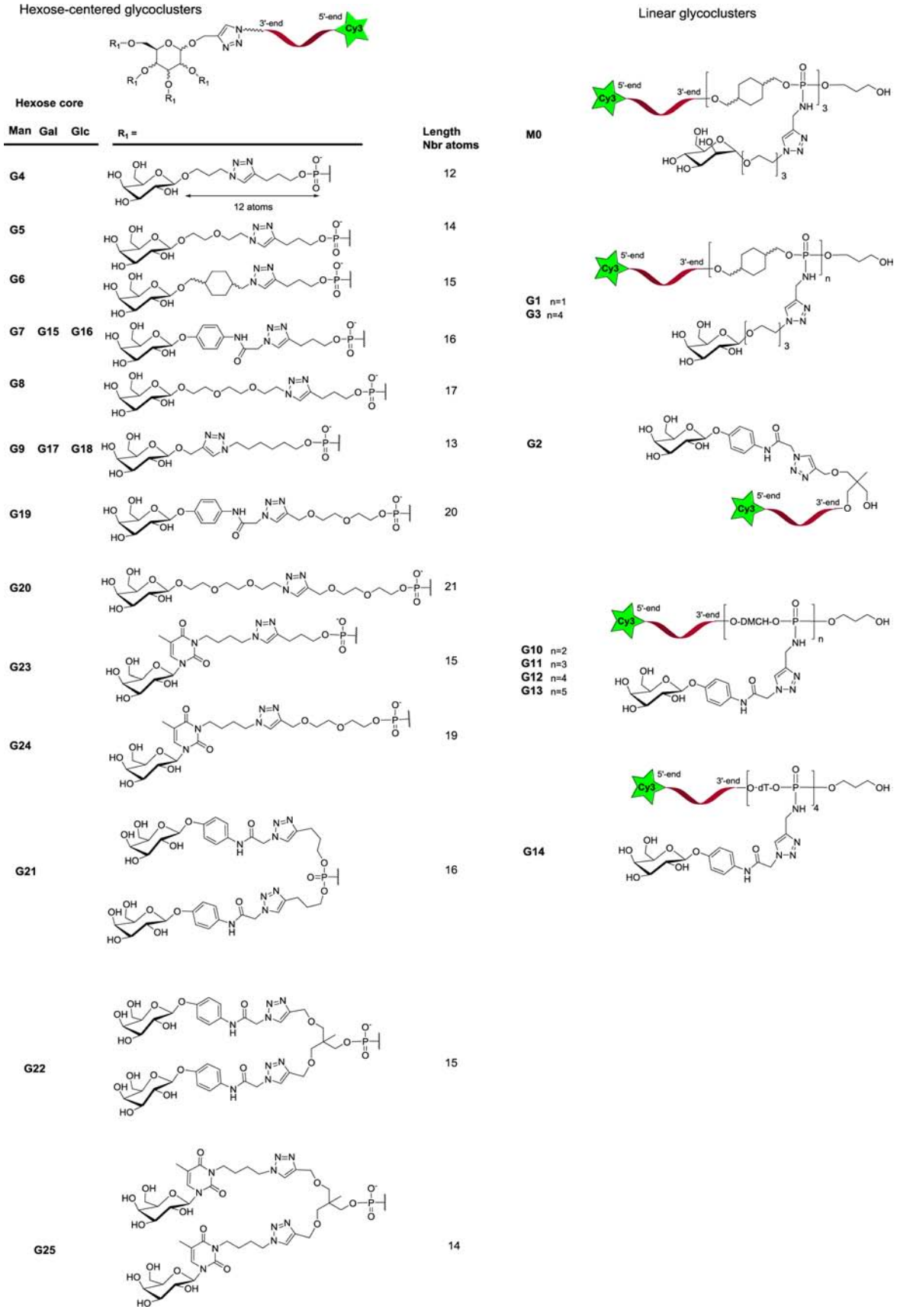

Figure 2. Structure of trimannosylated glycocluster **M0** and mono- to octa-galactosylated glycoclusters **G1-G25**.

IC_{50} values were determined using "BioDataFit 1.02 program". The model chosen was "Sigmoidal"

$$Y = a + (b - a)/[1 + 10^{(x-c)}]$$

dx.doi.org/10.1021/bc4005365 | *Bioconjugate Chem.* 2014, 25, 379−392

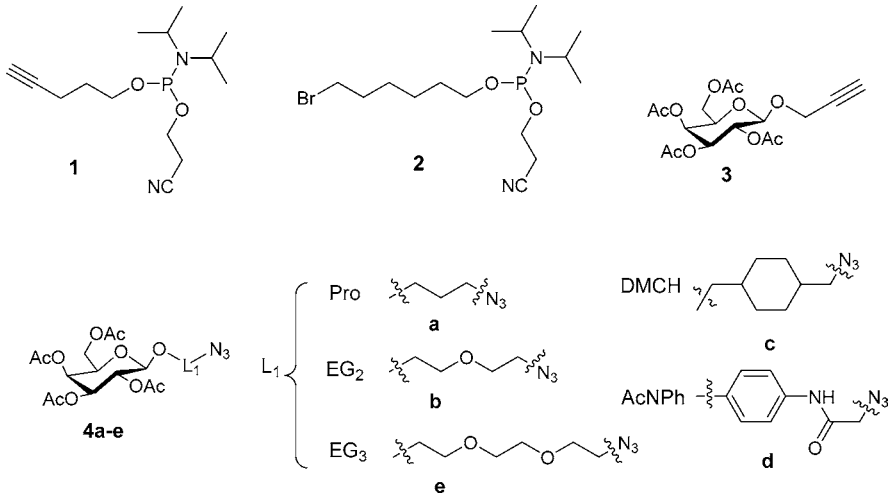

Figure 3. Building blocks for the synthesis of the galactoclusters.

with $a = FI_{min}$, $b = FI_{max}$, $x = \log[LecA]$, and $c = \log(IC_{50})$. $FI_{min/max}$ is the minimum/maximum Alexa-647 fluorescence signal observed for a galactomimetic.

RESULTS AND DISCUSSION

First, we synthesized mannose-centered glycoclusters (**G4**-**G9**) and studied the influence of six different linkers in glycomimetic on their recognition to LecA. The linkers were chosen to span different lengths (from 12 to 17 atoms calculated from the exoanomeric O1 of galactose to the phosphorus atom) and for their flexibility and solvation capacities (alkyl, aromatic, or ethylene glycol) (Figure 2).

To this end, we used two phosphoramidites (i.e., pent-4-ynyl **1** and 6-bromohexyl **2**) in combination with propagyl galactoside **3** and different galacto azide derivatives **4a**−**e** exhibiting different aglycones to construct the glycoclusters using phosphoramidite chemistry[41] and copper catalyzed azide alkyne cycloaddition (CuAAC) "click" chemistry[42,43] (Figure 3).

Propargyl galactoside **3** and galactose azide derivatives **4a**−**e** were prepared according to literature protocols.[18,30−34] The mannose-centered glycoclusters **G4**-**G9** were prepared according to our recently reported strategy.[29] Basically, propargyl α-D-mannopyranoside **6** was immobilized on an azide solid support **5** by CuAAC and then pent-4-ynyl **1** or bromohexyl **2** phosphoramidites were introduced on the four hydroxyls by phosphorylation affording the mannose core bearing four pentynylphosphate or four bromohexylphosphate groups (Scheme 1). The oligonucleotide was elongated and labeled with a fluorescent dye (Cy3) by classic phosphoramidite chemistry affording **8** or **9**. For **9**, the four bromine atoms were substituted with tetramethylguanidine azide (TMG N_3) to give the tetra azide oligonucleotide **10**. After an ammonia treatment, the compounds **11** and **12** were conjugated with galactose derivatives **4a**−**e** and **3**, respectively, by CuAAC in solution, using Cu(0) nanopowder, affording the mannose-centered tetra-galactosylated oligonucleotide conjugates **13a**−**e** and **14**. Pure conjugates were isolated by reverse phase HPLC and a final treatment with ammonia afforded the six expected tetragalactoclusters **G4**-**G9** exhibiting different linkers.

The binding efficiency of the galactomimetics **G4**-**G9** to LecA was determined using a DNA-based glycoarray by direct fluorescence scanning.[23] A linear trimannosylcluster (DMCH-$MTzEG_3$-Man)$_3$ **M0**[23] was used as negative control showing the specificity of LecA to galactoclusters. A linear tetragalactosylated cluster (DMCH-$MTzEG_3$-Gal)$_4$ **G3**[44] served as a positive control and comparison with the current tetravalent clusters (Figure 2). The nomenclature proposed for these glycoclusters is based on abbreviations of each building blocks.[22] To this purpose, all the glycoclusters were immobilized on a DNA-array by DNA directed immobilization (DDI) thanks to their complementary DNA tag. Then, Alexa 647-LecA was added and incubated for 3 h; after washing, the fluorescence intensity was read at 675 nm giving qualitative information on the binding strength (Figure 4). The linear trimannosylated glycocluster **M0** cluster did not bind to LecA showing the selective recognition and the absence of unspecific binding on the microarray. The linear tetragalactosylated cluster (DMCH-MTzEG3-Gal)$_4$ **G3** exhibited fluorescence around 3100 arbitrary unit (a.u.).

The data showed that there is no obvious correlation regarding the length of the linker between the galactose moiety and the mannose-core on the binding efficiency. Indeed, similarly to the work of Cecioni et al., it was found that increasing the flexible EG_2-based linker with 14 atoms in length in compound **G5** to the EG_3-based linker with 17 atoms in length in compound **G8** did not significantly improve the binding. Likewise, increasing the rigidity with linker DMCH in galactosylated cluster **G6** (15 atoms) did not result in improved binding to LecA.

In contrast, it appeared that galactomimetics with an aromatic group near the galactose moiety (**G7** and **G9**) showed high binding with a preference for the phenyl (AcNPh) moiety (**G7**) compared to the triazole methylene (TzM) motif (**G9**). Imberty et al. already observed this fact where a phenyl β-D-galactopyranoside presented a 26-fold increase of affinity to LecA compared to methyl β-D-galactopyranoside.[12] This could be explained by hydrophobic or $\pi-\pi$ interactions with aromatic amino acids of LecA near the CRD. This point was recently emphasized and it was demonstrated that aromatic aglycones present a CH−π "T-shaped" interaction with the His50 residue of the lectin.[45,46] The "aromatic" effect to increase the binding of carbohydrate to lectin has been previously observed for mannoside derivatives targeting mannose-specific protein FimH, which is expressed on the tips of type 1 fimbriae using mannoside monomers[47] or multivalent clusters.[48−50]

dx.doi.org/10.1021/bc4005365 | Bioconjugate Chem. 2014, 25, 379−392

Scheme 1. Synthesis of Glycoclusters G4-G9[a]

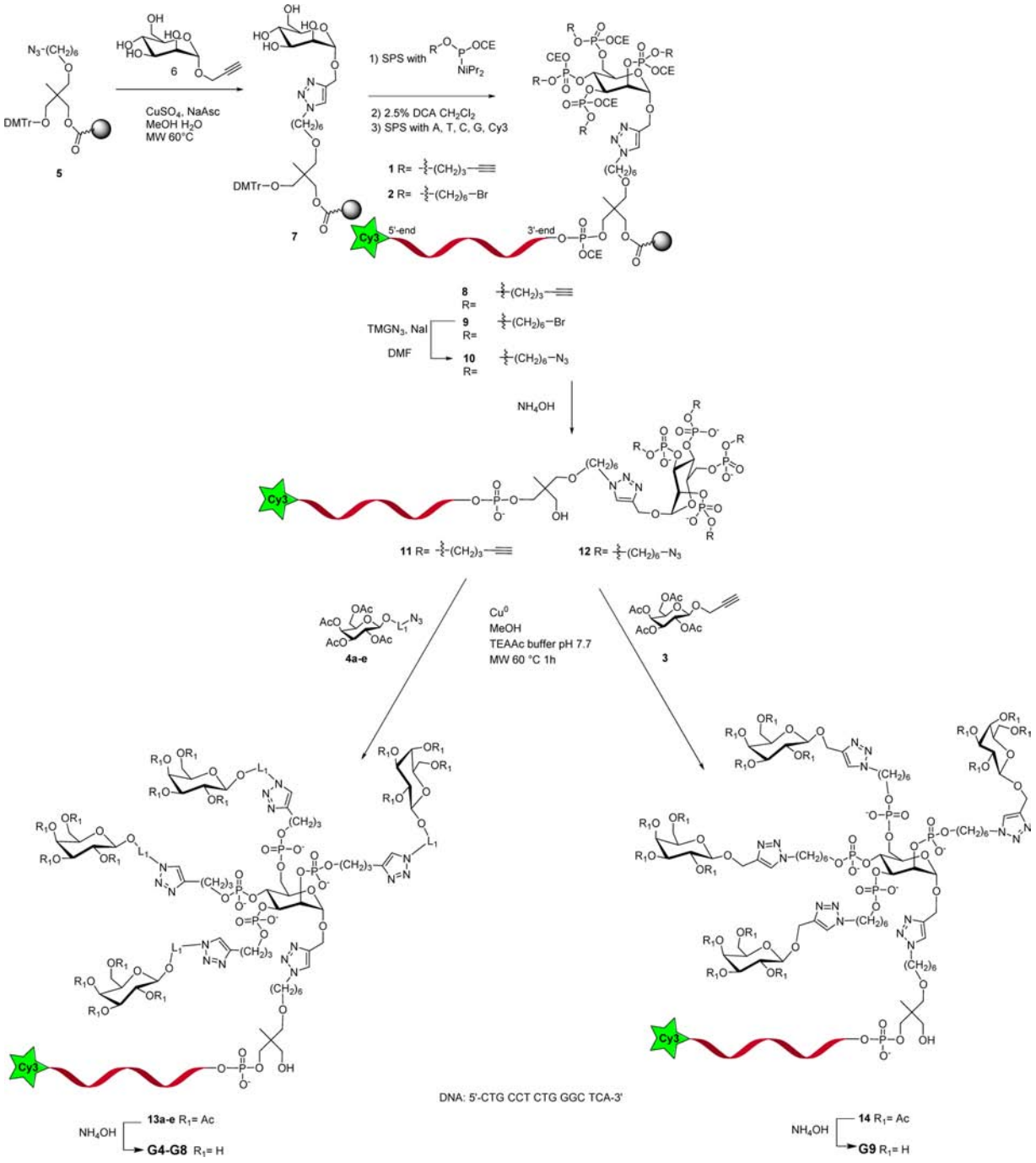

[a]L_1 are explained in Figure 2.

Interestingly, Roy et al. reported the same phenomenon that we observed with a higher increase of affinity with clusters exhibiting phenyl-*O*-mannopyranoside residues compared with those exhibiting triazolmethyl-*O*-mannopyranoside residues.[50]

The differences of binding between **G4**, **G5**, **G6**, and **G8** were not significant suggesting that ethylene glycol (EG_2 or EG_3) or aliphatic (Pro or DMCH) linkers did not interact further with amino acid residues of LecA.

In a second study, we looked at the effect of the AcNPh-galactose moiety on different scaffolds with, on one hand, its introduction into linear scaffolds like DMCH scaffold exhibiting two to five residues $(DMCH\text{-}MTzAcNPh\text{-}Gal)_{2-5}$ **G10-G13** or deoxythymidine scaffold exhibiting four galactose residues $(dT\text{-}MTzAcNPh\text{-}Gal)_4$ **G14** (Figure 2), and on the other hand the AcNPh-galactose moiety introduced into galactose- and glucose-centered scaffolds (**G15** and **G16**) (Figure 2). For comparison, the effect of HexTzM-galactose moiety was also studied with galactoclusters built on galactose- and glucose-centered scaffolds (**G17** and **G18**) (Figure 2).

The linear DMCH galactoclusters **G10-G13** were synthesized starting from the propanediol solid support on which DMCH *H*-phosphonate monoester[23,35] was coupled two to five times by *H*-phosphonate chemistry using pivaloyl chloride as

dx.doi.org/10.1021/bc4005365 | *Bioconjugate Chem.* 2014, 25, 379−392

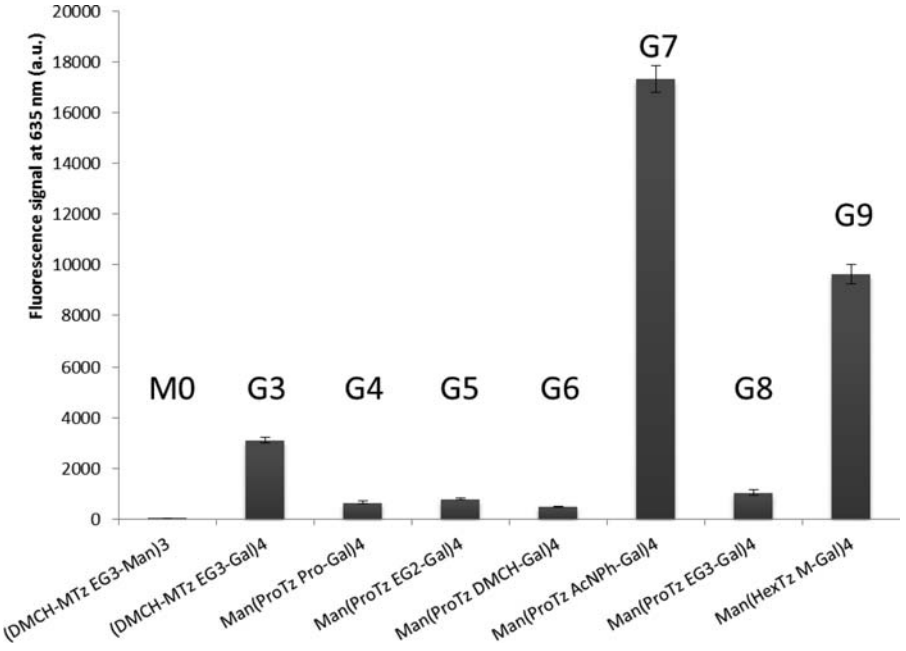

Figure 4. Fluorescence intensity (arbitrary units a.u.) of glycoclusters $(DMCH\text{-}MTzEG_3\text{-}Man)_3$ **M0**, $(DMCH\text{-}MTzEG_3\text{-}Gal)_4$ **G3**, and mannose-centered tetragalactocluster **G4-G9** bound with Alexa 647-PA-IL.

Scheme 2. Synthesis of Linear $(DMCH\text{-}MTzAcNPhGal)_{2\text{-}5}$ G10-G13 and $(dT\text{-}MTzAcNPhGal)_4$ G14 Clusters

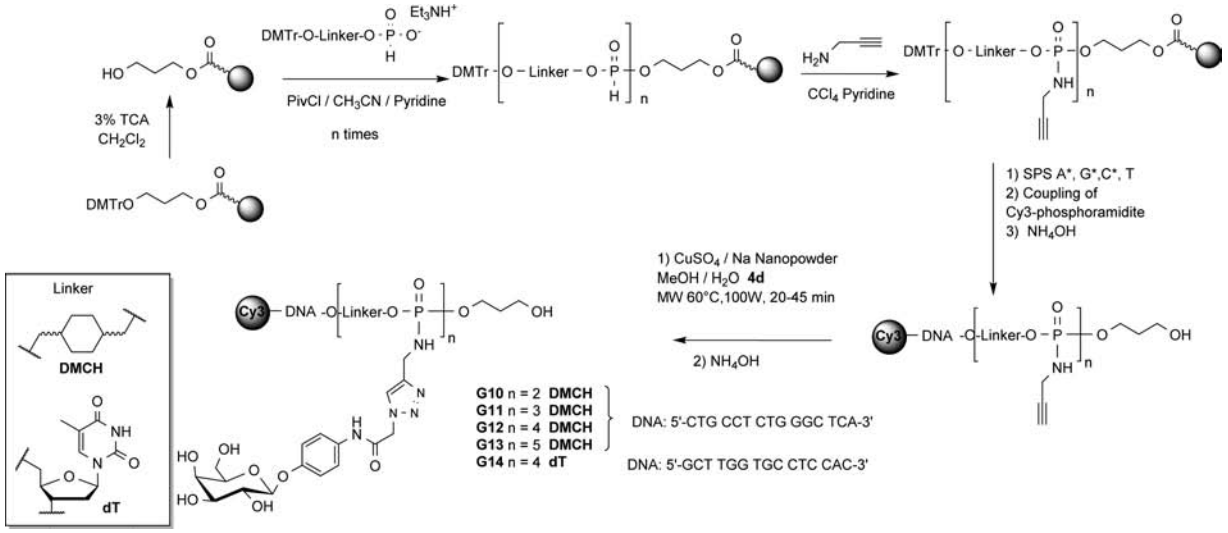

activator (Scheme 2).[27] The resulting *H*-phosphonate diester linkages were oxidized by carbon tetrachloride in the presence of propargyl amine allowing the introduction of alkyne functions. Then, the oligonucleotide was assembled and Cy3-labeled by phosphoramidite chemistry. After deprotection and release from the solid support, by ammonia treatment, the resulting modified oligonucleotides exhibiting two to five alkynes were conjugated with **4d** by CuAAC. After HPLC purification, the acetyl groups were removed by ammonia treatment leading to the oligonucleotides conjugated to linear DMCH galactoclusters **G10-G13**. The linear tetra-galactose on deoxythymidine scaffold $(dT\text{-}MTzAcNPhGal)_4$ **G14** was synthesized similarly using commercially available DMTr-thymidine *H*-phosphonate introduced four times on a 1,3-propanediol solid support.

The synthesis of galactose- and glucose-centered glycoclusters with $(proTzAcNPh\text{-}Gal)_4$ motif **G15** and **G16** and with $(HexTzM\text{-}Gal)_4$ motif **G17** and **G18** (Figure 2) proceeded using the same protocol as described above but using propargyl galactoside or propargyl glucoside, respectively, which were first immobilized on azide solid support **5**. In addition, for comparison purposes, an oligonucleotide conjugate exhibiting only one TzAcNPh-Gal motif **G2** was synthesized (Figure 2). To this end, a Cy3-oligonucleotide was synthesized from a monoalkyne solid support which was conjugated with **4d** by CuAAC affording **G2**.

The binding properties of these galactoclusters to LecA were studied using a DDI affording a glycoarray. After their immobilization on the chip and incubation with Alexa 647-LecA the fluorescence intensity of each glycocluster was read (Figure 5). The Alexa 647 fluorescent signal is therefore correlated to LecA binding. The fluorescent signal of the linear DMCH glycoclusters rose with the number of galactose residues showing the benefit of the increase of saccharide

dx.doi.org/10.1021/bc4005365 | *Bioconjugate Chem.* 2014, 25, 379−392

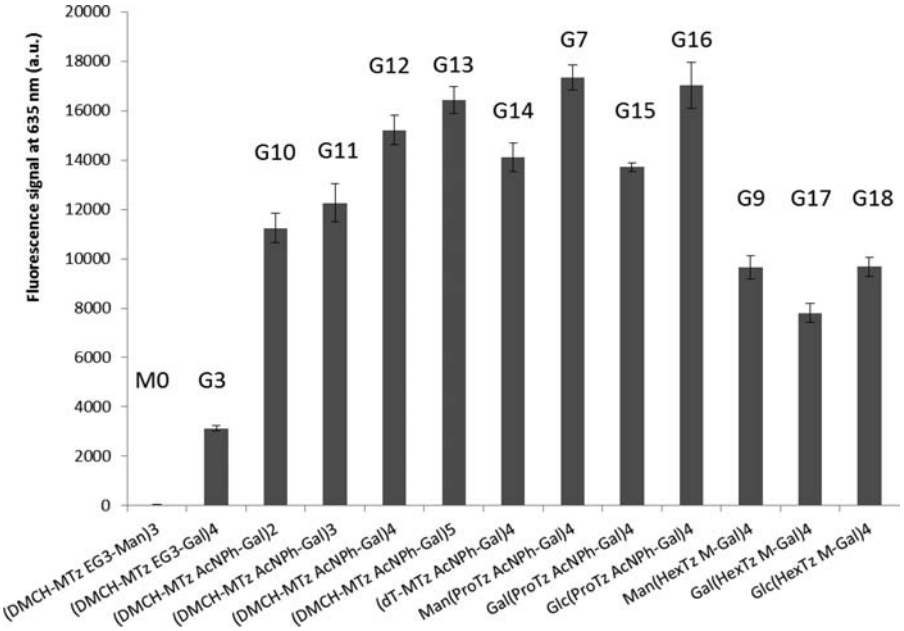

Figure 5. Fluorescence arbitrary unit (a.u.) of linear and hexose-centered glycoclusters **M0**, **G3**, $(DMCH\text{-}MTzAcNPh\text{-}Gal)_{2-5}$ **G10-G13**, $(dT\text{-}MTzAcNPh)_4$ **G14**, Man-, Gal-, Glc-$(ProTzAcNPh\text{-}Gal)_4$ **G7**, **G15**, **G16** and Man-, Gal-, Glc-$(HexTzM\text{-}Gal)_4$, **G9**, **G17**, **G18** bonded with Alexa 647-PA-IL.

Table 1. Names and Structures of Glycoclusters[a]

entry		glycoclusters	valency (N)	L_1	L_2	scaffold	IC_{50Lac} (μM)	potency (β)[b]	potency per residue (β/N)
1	**M0**	$(DMCH\text{-}MTzEG_3\text{-}Man)_3$	3	EG_3	M	DMCH			
				monovalent compounds					
2	**G1**	DMCH-MTz EG_3-Gal	1	EG_3	M	DMCH	5	1	1
3	**G2**	THME-MTzAcNPh-Gal	1	AcNPh	M	THME	16	3.2	3.2
				multivalent compounds					
4	**G4**	$Man(proTzPro\text{-}Gal)_4$	4	Pro	Pro	Man	nd	-	
5	**G5**	$Man(proTzEG_2\text{-}Gal)_4$	4	EG_2	Pro	Man	nd	-	
6	**G6**	$Man(proTzDMCH\text{-}Gal)_4$	4	DMCH	Pro	Man	nd	-	
7	**G7**	$Man(proTzAcNPh\text{-}Gal)_4$	4	AcNPh	Pro	Man	2826	565	141
8	**G8**	$Man(proTzEG_3\text{-}Gal)_4$	4	EG_3	Pro	Man	29	5.8	1.5
9	**G9**	$Man(HexTzM\text{-}Gal)_4$	4	M	Hex	Man	210	42	11
10	**G3**	$(DMCH\text{-}MTzEG_3\text{-}Gal)_4$	4	EG_3	M	DMCH	773	155	39
11	**G10**	$(DMCH\text{-}MTzAcNPh\text{-}Gal)_2$	2	AcNPh	M	DMCH	185	37	19
12	**G11**	$(DMCH\text{-}MTzAcNPh\text{-}Gal)_3$	3	AcNPh	M	DMCH	866	173	58
13	**G12**	$(DMCH\text{-}MTzAcNPh\text{-}Gal)_4$	4	AcNPh	M	DMCH	1056	211	53
14	**G13**	$(DMCH\text{-}MTzAcNPh\text{-}Gal)_5$	5	AcNPh	M	DMCH	1550	310	62
15	**G14**	$(dT\text{-}MTzAcNPh\text{-}Gal)_4$	4	AcNPh	M	dT	nd	-	-
16	**G15**	$Gal(ProTzAcNPh\text{-}Gal)_4$	4	AcNPh	Pro	Gal	662	132	33
17	**G16**	$Glc(ProTzAcNPh\text{-}Gal)_4$	4	AcNPh	Pro	Glc	805	161	40
18	**G17**	$Gal(HexTzM\text{-}Gal)_4$	4	M	Hex	Gal	532	106	27
19	**G18**	$Glc(HexTzM\text{-}Gal)_4$	4	M	Hex	Glc	775	155	39
20	**G19**	$Man(EG_2MTzAcNPh\text{-}Gal)_4$	4	AcNPh	EG_2M	Man	4218	844	211
21	**G20**	$Man(EG_2MTzEG_3\text{-}Gal)_4$	4	EG_3	EG_2M	Man	24	4.8	1.2
22	**G21**	$Man(proTzAcNPh\text{-}Gal)_8$	8	AcNPh	Pro	Man	6803	1361	170
23	**G22**	$Man[THME(MTzAcNPh\text{-}Gal)_2]_4$	8	AcNPh	THME(M)	Man	1807	361	45
24	**G23**	$Man(ProTzBuT\text{-}Gal)_4$	4	BuT	Pro	Man	nd	-	-
25	**G24**	$Man(EG2MTzBuT\text{-}Gal)_4$	4	BuT	EG_2M	Man	nd	-	-
26	**G25**	$Man[THME(MTzBuT\text{-}Gal)_2]_4$	8	BuT	THME(M)	Man	nd	-	-

[a] IC_{50Lac} values of the glycoclusters toward LecA determined by competition with lactose. Each glycocluster was immobilized on the surface by DDI and then Alexa647-LecA was added with an increasing concentration of lactose used as inhibitor. [b] The potency (β) was calculated using the monovalent DMCH-MTz-EG_3-Gal **G1** as a reference. nd not determined.

motifs on the binding efficiency. The tetracluster **G3** with $MTzEG_3$-Gal motifs displayed a fluorescence signal about 5-fold lower than its analog **G12** bearing TzAcNPh-Gal motifs confirming the better binding of phenylgalactoside. Both

dx.doi.org/10.1021/bc4005365 | Bioconjugate Chem. 2014, 25, 379−392

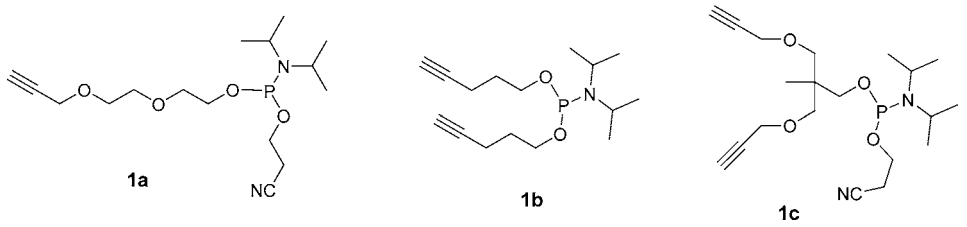

Figure 6. Structure of propargyl diethylene glycol, *bis*-pent-4-ynyl, and 2,2-(*bis*-propargyloxymethyl)propyl phosphoramidites.

Scheme 3. Synthesis of N^1-(2′,3′,4′,6′-tetra-*O*-acetyl-β-D-galactopyransosyl)-N^3-(4-azido-butyl)-thymine 4f

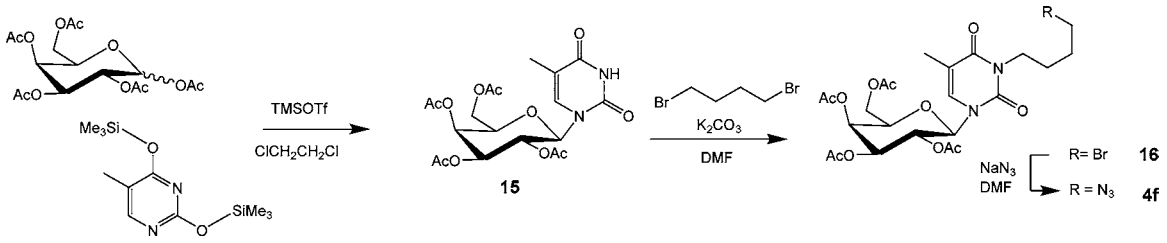

tetrameric linear glycoclusters with DMCH **G12** or thymidine scaffolds **G14** exhibited a higher binding than the DMCH trimeric cluster **G11** but with a preference for the DMCH one. Concerning the hexose-centered tetra-galactoclusters, the data confirmed the better binding of galactoclusters **G7**, **G15**, **G16** exhibiting ProTzAcNPh-Gal motifs versus HexTzM-Gal ones **G9**, **G17**, **G18** regardless of the hexose cores. For both families, glycoclusters built from a mannose- and glucose-core displayed similar fluorescent signal, and those built from a galactose-core displayed a lower signal (Figure 5).

The comparison between linear and hexose-centered glycoclusters bearing four ProTzAcNPh-Gal motifs gives the following increase of fluorescent signal: Gal(ProTzAcNPh-Gal)$_4$ **G15** ≤ (dT-MTzAcNPh-Gal)$_4$ **G14** < (DMCH-MTzAcNPh-Gal)$_4$ **G12** < (Glc(ProTzAcNPh-Gal)$_4$ **G16** ≤ Man(ProTzAcNPh-Gal)$_4$ **G7**. This data showed the better binding of mannose- and glucose-centered glycoclusters among all of the glycoclusters even better than the linear DMCH penta-galactose **G13**.

Since the dynamic range of fluorescent intensity is rather limited,[51,52] we then determined the IC_{50} value of the glycoclusters using lactose as inhibitor, and potency was calculated with respect to the monovalent galactose DMCH-MTzEG$_3$-Gal **G1** (Table 1). In our case, the IC_{50Lac} value corresponds to the lactose concentration required to displace 50% of LecA from the glycocluster. Hence, the higher the IC_{50Lac} value, the higher the affinity of the glycocluster for LecA.

The comparison of the monogalactoses DMCH-MTz-EG$_3$-Gal **G1**[23] and MTzAcNPh-Gal **G2** with IC_{50Lac} values of 5 and 16 μM, respectively, showed a 3.2-fold increase of binding for the aromatic galactose (Entries 2 and 3), which is similar to the observation made by Cecioni et al. by enzyme linked lectin assay[18] (ELLA), the most similar method used in that report in comparison to our carbohydrate microarray technique. For the linear galactoclusters, we observed an increase of IC_{50Lac} value corresponding to a better binding to LecA with the increase in the number of residues with a threshold effect between 2 and 3 residues (Table 1, entries 11 and 12). The benefit of the aromatic (MTzAcNPh) linker versus MTzEG$_3$ linker was confirmed with linear DMCH clusters: (DMCH-MTzAcNPh-Gal)$_4$ **G12** (entry 13: IC_{50Lac} = 1056 μM, β = 211) versus (DMCH-MTzEG$_3$-Gal)$_4$ **G3** (entry 10: IC_{50Lac} = 773 μM, β = 155). This trend was even more important for the mannose-centered glycoclusters Man(ProTzEG$_3$-Gal)$_4$ **G8** (entry 8: IC_{50Lac} = 29 μM, β = 5.8) versus Man(ProTzAcNPh-Gal)$_4$ **G7** (entry 7: IC_{50Lac} = 2826 μM and β = 565). The results indicated the superiority of a TzAcNPh-Gal motif in comparison with TzEG$_3$-Gal with an increase in potency of almost 100-fold in this multivalent presentation.

Surprisingly, the data showed that the influence of hexose-core on the binding to LecA is different according to the nature of the galactose-linkers (Table 1). Concerning the tetragalactoclusters, with a ProTzAcNPh linker, the best binding was observed for the mannose-core **G7** followed by the glucose-**G16** and the galactose-**G15** cores (entries 7, 17, 16). In contrast, with a HexTzM linker, the best binding was observed for the cluster with a glucose-core **G18** followed by the galactose-**G17** and mannose- **G9** core (entries 19, 18, 9).These results illustrate that the combination of the nature of the linker and the spatial arrangement has a strong influence on the affinity toward LecA.

In a third optimization, we decided to keep a mannose core and the aromatic TzAcNPh-Gal motifs with some variations. On one hand, we increased the length/flexibility between the mannose-core and the triazole using a diethylene glycol propargyl phosphoramidite **1a**[27] instead of the pent-4-ynyl one, and on the other hand, we introduced eight alkynyl groups using either a *bis*-pent-4-ynyl phosphoramidite **1b**[27] or a 2,2-(*bis*-propargyloxymethyl)propyl phosphoramidite **1c**[28] (Figure 6). Thus, the new mannose-centered tetragalactoclusters Man(EG$_2$MTzAcNPh-Gal)$_4$ **G19** exhibit a 20 atom linker length instead of 16 atoms for Man(ProTzAcNPh-Gal)$_4$ **G7**. The mannose-centered octagalactoclusters Man(ProTzAcNPh-Gal)$_8$ **G21** and Man[THME(MTzAcNPh-Gal)$_2$]$_4$ **G22** exhibit two residues on each hydroxyl of the mannose-core (Figure 2). So, we could evaluate the influence of the linker length and the influence of the number of residues on the binding properties. For comparison purposes, we also synthesized the analogue Man(EG$_2$MTzEG$_3$-Gal)$_4$ **G20** in which aromatic AcNPh-Gal motifs were replaced by EG$_3$-Gal motifs (Figure 2).

Finally, to gain more insight from an "aromatic effect", we synthesized new glycoclusters **G23**-**G25** exhibiting galactose motifs where the *O*-phenyl was replaced by a thymine affording a N^1-thymidine-β-galactopyranoside derivative (T-Gal)

dx.doi.org/10.1021/bc4005365 | *Bioconjugate Chem.* 2014, 25, 379−392

Scheme 4. Synthesis of Man(EG_2MTzAcNPh-Gal)$_4$ G19, Man(EG_2MTzEG$_3$-Gal)$_4$ G20, Man(ProTzAcNPh-Gal)$_8$ G21, Man[THME(MTzAcNPh-Gal)$_2$]$_4$ G22, Man(ProTzBuT-Gal)$_4$ G23, Man(EG_2MTzBuT-Gal)$_4$ G24, and Man[THME(MTzBuT-Gal)$_2$]$_4$ G25

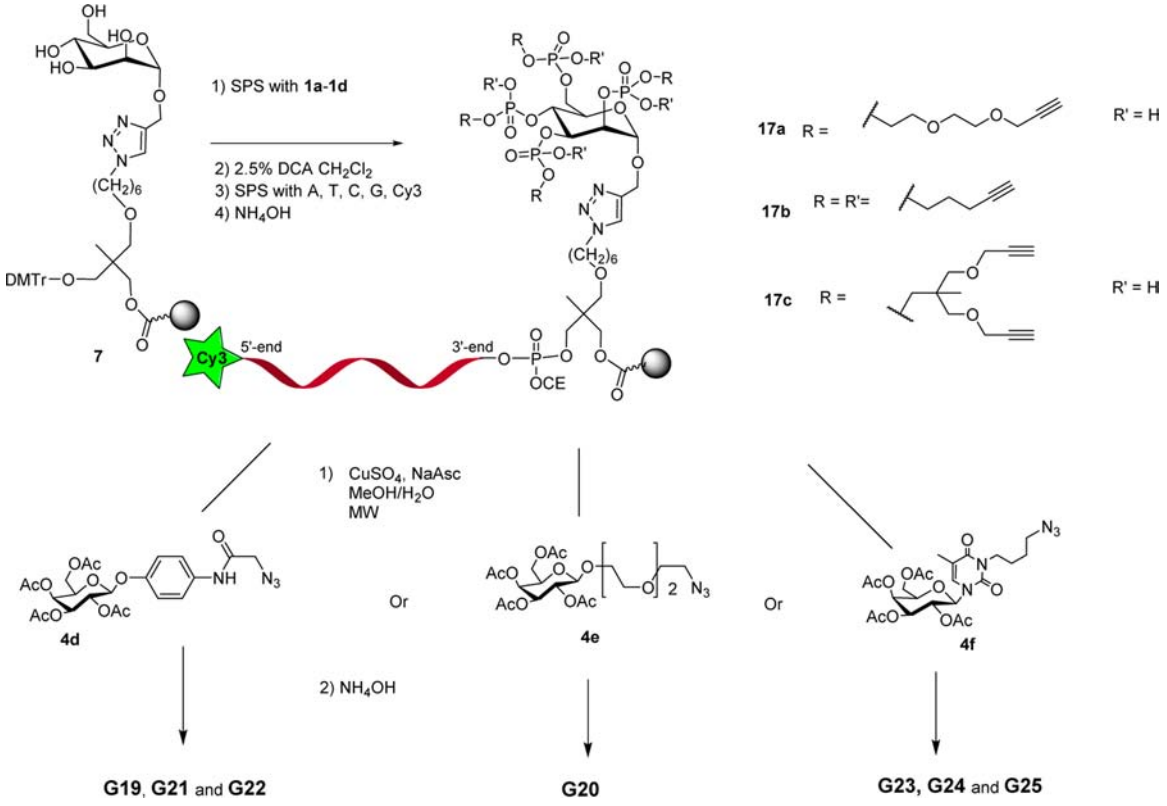

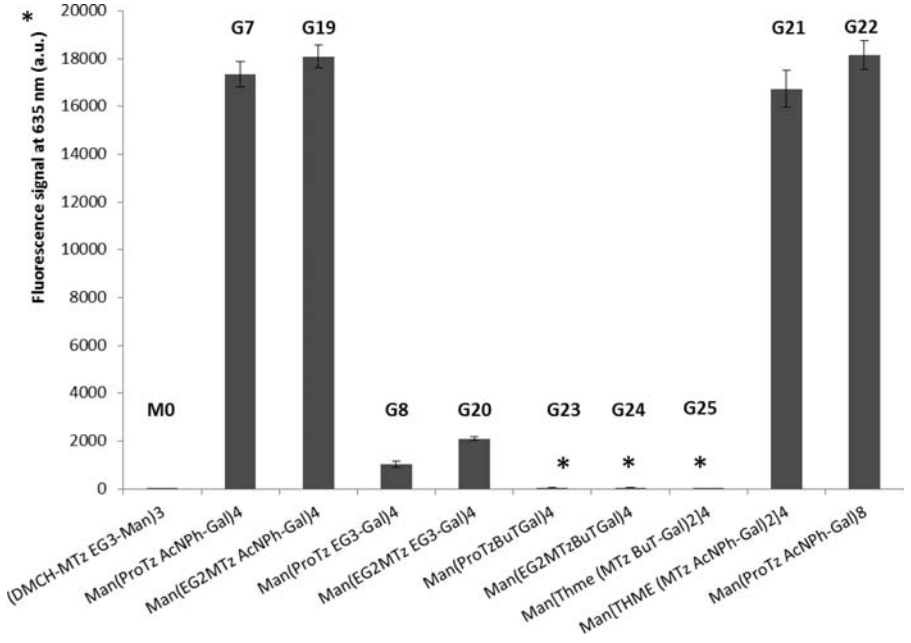

Figure 7. Fluorescence arbitrary unit (a.u.) of linear and hexose-centered glycoclusters bonded with Alexa647-LecA. * a.u. between 41 and 45.

(Scheme 3). This analogue was designed to may form additional hydrogen bonds between the heteroatoms of the thymine and the amino acid of the lectin leading to a possible better affinity. To this end, the azide derivative **4f** was prepared according to a protocol described in the literature for the synthesis of glucose-thymidine.[53] The 1,2,3,4,6-penta-*O*-acetyl-D-galactopyranose was glycosylated with 2,4-bis-*O*-trimethylsilyl-thymine affording the N^1-(2′,3′,4′,6′-tetra-*O*-acetyl-*β*-D-galactopyranosyl)-thymine **15** (T-Gal) (Scheme 3). It was further alkylated with 1,4-dibromobutane on the N^3 of the thymine moiety in the presence of potassium carbonate leading to **16**, and finally, the bromine atom was substituted by sodium azide affording the corresponding azide N^1-thymine-galactose derivative (BuT-Gal) **4f**.

dx.doi.org/10.1021/bc4005365 | *Bioconjugate Chem.* 2014, 25, 379−392

For the synthesis of the new glycoclusters exhibiting either AcNPh-Gal or BuT-Gal motifs, the solid-supported mannose **7** was phosphorylated using either diethylene glycol propargyl phosphoramidite (**1a**), *bis*-pent-4-ynyl phosphoramidite (**1b**), or 2,2-(*bis*-propargyloxymethyl)propyl phosphoramidite (**1c**) (Scheme 4). Then, after oligonucleotide elongation and labeling, the tetra/octa alkyne constructions (**17a−c**) were conjugated to **4d** affording the expected mannose-centered tetra/octagalactocluster oligonucleotide conjugates Man-$(EG_2MTzAcNPh\text{-}Gal)_4$ **G19**, $Man(ProTzAcNPh\text{-}Gal)_8$ **G21**, and $Man[THME(MTzAcNPh\text{-}Gal)_2]_4$ **G22**, respectively, after ammonia treatment. Likewise, the tetraalkyne **17a** with diethylene glycol propargyl linkers was also conjugated with **4e** affording the $Man(EG_2MTzEG_3\text{-}Gal)_4$ **G20**. For the T-Gal clusters, the Gal-T azide derivative **4f** was conjugated with the mannose-core exhibiting four pentynyl (**11**), four diethylene glycol propargyl (**17a**), or four *bis*-propargyl-oxymethyl propyl (**17c**) leading to tetraclusters with ProTzBuT-Gal or $EG_2MTzBuT\text{-}Gal$ motifs, respectively, and an octagalactocluster with THMEMTzBuTGal motif affording the expected mannose-centered tetra/octagalactocluster oligonucleotide conjugates $Man(ProTzBuT\text{-}Gal)_4$ **G23**, $Man(EG_2MTzBuT\text{-}Gal)_4$ **G24**, and $Man[THME(MTzBuT\text{-}Gal)_2]_4$ **G25** (Figure 2).

The binding for LecA of the eight resulting glycoclusters was determined by DDI-microarray as described above (Figure 7). The increase of the length of the linker from Pro (**G7**, **G8**) to EG_2M (**G19**, **G20**) led to a slight increase of affinity with both $TzEG_3$-Gal and TzAcNPh-Gal motifs with a consistently better affinity for the glycoclusters **G7** and **G19** with the aromatic motif (TzAcNPh-Gal).

For the $Man(ProTzAcNPh\text{-}Gal)_{4/8}$ **G7** and **G21** clusters, the increase in the number of residues from 4 to 8 led to a slight increase of fluorescent signal [$Man(ProTzAcNPh\text{-}Gal)_4$ **G7** vs $Man(ProTzAcNPh\text{-}Gal)_8$ **G21**]. However, the fluorescent signal of the octacluster was similar to that of the tetracluster with EG_2M linkers. In contrast, the other octacluster Man-$[THME(MTzAcNPh\text{-}Gal)_2]_4$ **G22** displayed a lower fluorescent signal than the two best tetraclusters. Concerning the galactoclusters made from BuT-Gal **G23-G25**, we observed a 635 fluorescent signal of about 45 a.u., very similar to the negative control. Increasing the number of galactoside residues to 8 did not give any improvement in the binding. The reasons for the inhibition of binding to LecA for thymine galactoside clusters may be related to detrimental steric hindrance considerations, since the thymine is directly connected to the C1 of galactopyranose that prevents the galactose moiety from entering into the binding site of LecA. This result is similar to the finding of Moni et al.,[51] where the binding of LecA to tetragalactose calixarene clusters was impaired due to the vicinity of the triazole ring. Indeed, in this study, the triazole ring was directly attached to the anomeric carbon of the *C*-galactoside. These results indicate that aromatic moieties must be connected with the galactose through at least one atom. The octagalactocluster $Man(ProTzAcNPh\text{-}Gal)_8$ **G22** exhibited the highest binding of all the constructions reported so far showing a better cluster effect due to the higher number of galactose motifs.

For a better understanding of the binding properties, we measured the IC_{50Lac} value of the glycoclusters (Table 1, entries 20−23). The potency of each galactocluster was calculated according to mono-EG_3-galactose **G1**. The IC_{50Lac} values confirmed the trends observed by direct fluorescence scanning with a better binding from $TzEG_3$-Gal **G20** to TzAcNPh-Gal **G19** motifs (entry 21 vs entry 20) and a better binding due to the elongation of the linker from Pro to EG_2M (entry 8 vs entry 21 and entry 7 vs entry 20). The tetragalactocluster **G19** with the longest linker exhibited the highest relative potency per residues of 211-fold (entry 20). The highest binding was found for the octaglycocluster **G21** with ProTzAcNPh-Gal motifs (IC_{50Lac} = 6803 μM, β = 1361, entry 22). The comparison of the potency per residues between this octacluster **G21** versus the tetragalactose **G7** with the same linker ProTzAcNPh still showed an increase of binding of 30-fold (170 and 141, respectively, entry 22 versus entry 7) demonstrating the advantage of the increase in valency. In contrast, the second octagalactocluster **G22** displayed a lower IC_{50Lac} value of 1807 μM and β = 361 (entry 23) than the tetragalactoclusters with ProTzAcNPh and $EG_2MTzAcNPh$ linkers, **G7** and **G19**, respectively, showing that the spatial arrangement has a strong effect on the binding.

In conclusion, thanks to this strategy combining nucleic acid chemistry and CuAAC chemistry, we were able to synthesize rapidly 25 galactoclusters, at nanomolar scale, with different number of residues and different topologies, and to evaluate their binding for LecA using a DDI-glycoarray requiring only few picomoles of sample. Among them, linear galactoclusters with DMCH scaffold and 3 to 5 aromatic (TzAcNPh-Gal) motifs (**G11-G13**) exhibited an increase of potency of 173-, 211-, and 310-fold, respectively, in comparison with the mono $TzEG_3$-Gal motif (**G1**). Furthermore, we found that two mannose-centered tetragalactoclusters with aromatic motifs and with linker of 16- (**G7**) and 20-atom (**G19**) lengths exhibited better affinity with potency increased by 565-fold and 844-fold, respectively. Finally, the mannose-centered octagalactocluster [$Man(ProTzAcNPh\text{-}Gal)_8$] (**G21**) with aromatic motifs and a linker of 16 atom length displayed the best affinity with a 1361-fold increase of potency. As a rule, we confirmed the benefit of the "aromatic" effect of galactoclusters to reach high affinity toward LecA regardless of the scaffold. However, the scaffold is also an important factor to have high affinity; thus, the mannose core was preferred to galactose or glucose. The increase of length between the mannose core and the peripheral galactose is also a factor to improve the binding to LecA.

These very promising results prompt us to synthesize the "hit" galactoclusters without the DNA tag on a ∼100 mg scale for the evaluation of their affinity by more classical methods (i.e., HIA, SPR, ELLA, and ITC) and for their biological evaluation on whole *Pseudomonas aeruginosa* as potential anti-adhesive or anti-biofilm agents.

■ ASSOCIATED CONTENT

Supporting Information

General procedures, HPLC and MS data of galactomimetics, NMR data of compounds **15** and **16**, **4f**.This material is available free of charge via the Internet at http://pubs.acs.org.

■ AUTHOR INFORMATION

Corresponding Authors

*Tel.: +33/467 144 961; fax: +33/467 042 029; e-mail: morvan@univ-montp2.fr.

*Tel: +33/472 186 240, fax: +33/4 78 43 35 93, e-mail: yann.chevolot@ec-lyon.fr.

Notes

The authors declare no competing financial interest.

■ ACKNOWLEDGMENTS

This work was financially supported by ANR-12-BSV5-0020, Lyon Biopole, Plateform NanoLyon is acknowledged for its technical support. G.P. thanks the CNRS and the Région Languedoc-Roussillon for the award of a research studentship. C. L. thanks University of Montpellier 2 for a research studentship. F.M. is member of Inserm.

■ REFERENCES

(1) Floret, N., Bertrand, X., Thouverez, M., and Talon, D. (2009) Nosocomial infections caused by Pseudomonas aeruginosa: Exogenous or endogenous origin of this bacterium? *Pathol. Biol. 57*, 9−12.

(2) Lyczak, J. B., Cannon, C. L., and Pier, G. B. (2002) Lung infections associated with cystic fibrosis. *Clin. Microbiol. Rev. 15*, 194−222.

(3) Bernardi, A., Jimenez-Barbero, J., Casnati, A., De Castro, C., Darbre, T., Fieschi, F., Finne, J., Funken, H., Jaeger, K. E., Lahmann, M., Lindhorst, T. K., Marradi, M., Messner, P., Molinaro, A., Murphy, P. V., Nativi, C., Oscarson, S., Penades, S., Peri, F., Pieters, R. J., Renaudet, O., Reymond, J. L., Richichi, B., Rojo, J., Sansone, F., Schaffer, C., Turnbull, W. B., Velasco-Torrijos, T., Vidal, S., Vincent, S., Wennekes, T., Zuilhof, H., and Imberty, A. (2013) Multivalent glycoconjugates as anti-pathogenic agents. *Chem. Soc. Rev. 42*, 4709−4727.

(4) Chabre, Y. M., and Roy, R. (2013) Multivalent glycoconjugate syntheses and applications using aromatic scaffolds. *Chem. Soc. Rev. 42*, 4657−4708.

(5) Reymond, J. L., Bergmann, M., and Darbre, T. (2013) Glycopeptide dendrimers as Pseudomonas aeruginosa biofilm inhibitors. *Chem. Soc. Rev. 42*, 4814−4822.

(6) Garber, N., Guempel, U., Belz, A., Gilboagarber, N., and Doyle, R. J. (1992) On the specificity of the D-galactose-binding lectin (PA-I) of Pseudomonas aeruginosa and its strong binding to hydrophobic derivatives of D-galactose and thiogalactose. *Biochim. Biophys. Acta 1116*, 331−333.

(7) Chemani, C., Imberty, A., de Bentzmann, S., Pierre, M., Wimmerova, M., Guery, B. P., and Faure, K. (2009) Role of LecA and LecB lectins in Pseudomonas aeruginosa-induced lung injury and effect of carbohydrate ligands. *Infect. Immun. 77*, 2065−2075.

(8) Diggle, S. P., Stacey, R. E., Dodd, C., Camara, M., Williams, P., and Winzer, K. (2006) The galactophilic lectin, LecA, contributes to biofilm development in Pseudomonas aeruginosa. *Environ. Microbiol. 8*, 1095−1104.

(9) Bajolet-Laudinat, O., Girod-de Bentzmann, S., Tournier, J. M., Madoulet, C., Plotkowski, M. C., Chippaux, C., and Puchelle, E. (1994) Cytotoxicity of Pseudomonas-aeruginosa internal lectin Pa-I to respiratory epithelial-cells in primary culture. *Infect. Immun. 62*, 4481−4487.

(10) Laughlin, R. S., Musch, M. W., Hollbrook, C. J., Rocha, F. M., Chang, E. B., and Alverdy, J. C. (2000) The key role of Pseudomonas aeruginosa PA-I lectin on experimental gut-derived sepsis. *Ann. Surg. 232*, 133−142.

(11) Cioci, G., Mitchell, E. P., Gautier, C., Wimmerova, M., Sudakevitz, D., Perez, S., Gilboa-Garber, N., and Imberty, A. (2003) Structural basis of calcium and galactose recognition by the lectin PA-IL of Pseudomonas aeruginosa. *FEBS Lett. 555*, 297−301.

(12) Imberty, A., Wimmerova, M., Mitchell, E. P., and Gilboa-Garber, N. (2004) Structures of the lectins from Pseudomonas aeruginosa: insights into the molecular basis for host glycan recognition. *Microb. Infect. 6*, 221−228.

(13) Chen, C. P., Song, S. C., Gilboa-Garber, N., Chang, K. S. S., and Wu, A. M. (1998) Studies on the binding site of the galactose-specific agglutinin PA-IL from Pseudomonas aeruginosa. *Glycobiology 8*, 7−16.

(14) Lis, H., and Sharon, N. (1998) Lectins: carbohydrate-specific proteins that mediate cellular recognition. *Chem. Rev. 98*, 637−674.

(15) Lundquist, J. J., and Toone, E. J. (2002) The cluster glycoside effect. *Chem. Rev. 102*, 555−578.

(16) Lee, Y. C., and Lee, R. T. (1995) Carbohydrate-protein interactions: basis of glycobiology. *Acc. Chem. Res. 28*, 321−327.

(17) Morvan, F., Vidal, S., Souteyrand, E., Chevolot, Y., and Vasseur, J. J. (2012) DNA glycoclusters and DNA-based carbohydrate microarrays: From design to applications. *RSC Adv. 2*, 12043−12068.

(18) Cecioni, S., Praly, J. P., Matthews, S. E., Wimmerova, M., Imberty, A., and Vidal, S. (2012) Rational design and synthesis of optimized glycoclusters for multivalent lectin-carbohydrate interactions: influence of the linker arm. *Chem.—Eur. J. 18*, 6250−6263.

(19) Reynolds, M., Marradi, M., Imberty, A., Penades, S., and Perez, S. (2012) Multivalent gold glycoclusters: high affinity molecular recognition by bacterial lectin PA-IL. *Chem.—Eur. J. 18*, 4264−4273.

(20) Goudot, A., Pourceau, G., Meyer, A., Gehin, T., Vidal, S., Vasseur, J. J., Morvan, F., Souteyrand, E., and Chevolot, Y. (2013) Quantitative analysis (Kd and IC50) of glycoconjugates interactions with a bacterial lectin on a carbohydrate microarray with DNA Direct Immobilization (DDI). *Biosens. Bioelectron. 40*, 153−160.

(21) Pertici, F., and Pieters, R. J. (2012) Potent divalent inhibitors with rigid glucose click spacers for Pseudomonas aeruginosa lectin LecA. *Chem. Commun. 48*, 4008−4010.

(22) Nomenclature used for the Glycoclusters: Each glycocluster is constituted of a scaffold, a linker L_2, a triazole (Tz), and a linker L_1: Scaffold-L_2-Tz-L_1-carbohydrate. The linker L_1 corresponds to the aglycone motif of the carbohydrate without the azide or alkyne function and the linker L_2 corresponds to the linker (without the phosphorous moiety) between the scaffold and the triazole ring. Scaffolds used DMCH (dimethylcyclohexane), Man (mannose), Gal (galactose), Glc (glucose), or dT (thymidine), L_1: Pro (propyl), EG_2 (diethylene glycol), EG_3 (triethylene glycol), DMCH (1,4-dimethyl-cyclohexan), AcNPh (acetamidephenyl), M (methylene), BuT (N^3-butyl-thymine), L_2: Pro, Hex (hexyl) EG_2M (diethylene glycol methylene), THME tris-(hydroxymethyl)ethane. For example, cluster **G7** named Man(ProTzAcPh-Gal)$_4$ means that it has a mannose (Man) core connected to four peripheral galactose (Gal)$_4$ through a linker formed with a propyl (Pro) a triazole (Tz) and an acetamidephenyl (AcNPh). Linear glycoclusters have phosphoramidate linkages and hexose-centered ones have phosphate linkages. The generic terms of galactosylated clusters or galactoclusters were used to indicate that carbohydrates involved in the recognition with LecA are galactose residues. Obviously, galactoclusters built from a mannoside or glucoside core are not pure galactoclusters.

(23) Chevolot, Y., Bouillon, C., Vidal, S., Morvan, F., Meyer, A., Cloarec, J. P., Jochum, A., Praly, J. P., Vasseur, J. J., and Souteyrand, E. (2007) DNA-based carbohydrate biochips: A platform for surface glyco-engineering. *Angew. Chem., Int. Ed. 46*, 2398−2402.

(24) Meyer, A., Pourceau, G., Vasseur, J. J., and Morvan, F. (2010) 5′-Bis-conjugation of oligonucleotides by amidative oxidation and click chemistry. *J. Org. Chem. 75*, 6689−6692.

(25) Lietard, J., Meyer, A., Vasseur, J. J., and Morvan, F. (2008) New strategies for cyclization and bicyclization of oligonucleotides by click chemistry assisted by microwaves. *J. Org. Chem. 73*, 191−200.

(26) Lietard, J., Meyer, A., Vasseur, J. J., and Morvan, F. (2007) An efficient reagent for 5′-azido oligonucleotide synthesis. *Tetrahedron Lett. 48*, 8795−8798.

(27) Gerland, B., Goudot, A., Pourceau, G., Meyer, A., Dugas, V., Cecioni, S., Vidal, S., Souteyrand, E., Vasseur, J. J., Chevolot, Y., and Morvan, F. (2012) Synthesis of a library of fucosylated glycoclusters and determination of their binding toward Pseudomonas aeruginosa Lectin B (PA-IIL) using a DNA-based carbohydrate microarray. *Bioconjugate Chem. 23*, 1534−1547.

(28) Ligeour, C., Meyer, A., Vasseur, J. J., and Morvan, F. (2012) Bis- and tris-alkyne phosphoramidites for multiple 5′-labeling of oligonucleotides by click chemistry. *Eur. J. Org. Chem.*, 1851−1856.

(29) Pourceau, G., Meyer, A., Chevolot, Y., Souteyrand, E., Vasseur, J. J., and Morvan, F. (2010) Oligonucleotide carbohydrate-centered galactosyl cluster conjugates synthesized by click and phosphoramidite chemistries. *Bioconjugate Chem. 21*, 1520−1529.

(30) Hasegawa, T., Numata, M., Okumura, S., Kimura, T., Sakurai, K., and Shinkai, S. (2007) Carbohydrate-appended curdlans as a new

family of glycoclusters with binding properties both for a polynucleotide and lectins. *Org. Biomol. Chem. 5*, 2404−2412.
(31) Joosten, J. A. F., Loimaranta, V., Appeldoorn, C. C. M., Haataja, S., El Maate, F. A., Liskamp, R. M. J., Finne, J., and Pieters, R. J. (2004) Inhibition of Streptococcus suis adhesion by dendritic galabiose compounds at low nanomolar concentration. *J. Med. Chem. 47*, 6499−6508.
(32) Szurmai, Z., Szabo, L., and Liptak, A. (1989) Diethylene and triethylene glycol spacers for the preparation of neoglycoproteins. *Acta Chim. Hung. 126*, 259−269.
(33) Pourceau, G., Meyer, A., Vasseur, J. J., and Morvan, F. (2009) Synthesis of mannose and galactose oligonucleotide conjugates by Bi-click chemistry. *J. Org. Chem. 74*, 1218−1222.
(34) Mereyala, H. B., and Gurrala, S. R. (1998) A highly diastereoselective, practical synthesis of allyl, propargyl 2,3,4,6-tetra-*O*-acetyl-beta-D-gluco, beta-D-galactopyranosides and allyl, propargyl heptaacetyl-beta-D-lactosides. *Carbohydr. Res. 307*, 351−354.
(35) Bouillon, C., Meyer, A., Vidal, S., Jochum, A., Chevolot, Y., Cloarec, J. P., Praly, J. P., Vasseur, J. J., and Morvan, F. (2006) Microwave assisted ″click″ chemistry for the synthesis of multiple labeled-carbohydrate oligonucleotides on solid support. *J. Org. Chem. 71*, 4700−4702.
(36) Mazurczyk, R., Khoury, G. E., Dugas, V., Hannes, B., Laurenceau, E., Cabrera, M., Krawczyk, S., Souteyrand, E., Cloarec, J. P., and Chevolot, Y. (2008) Low-cost, fast prototyping method of fabrication of the microreactor devices in soda-lime glass. *Sens. Actuators, B 128*, 552−559.
(37) Vieillard, J., Mazurczyk, R., Morin, C., Hannes, B., Chevolot, Y., Desbène, P.-L., and Krawczyk, S. (2007) Application of microfluidic chip with integrated optics for electrophoretic separations of proteins. *J. Chromatogr., B 845*, 218−225.
(38) Dugas, V., and Chevalier, Y. (2003) Surface hydroxylation and silane grafting on fumed and thermal silica. *J. Colloid Interface Sci. 264*, 354−361.
(39) Dugas, V., Depret, G., Chevalier, B., Nesme, X., and Souteyrand, E. (2004) Immobilization of single-stranded DNA fragments to solid surfaces and their repeatable specific hybridization: covalent binding or adsorption? *Sens. Actuators, B 101*, 112−121.
(40) Blanchard, B., Nurisso, A., Hollville, E., Tetaud, C., Wiels, J., Pokorna, M., Wimmerova, M., Varrot, A., and Imberty, A. (2008) Structural basis of the preferential binding for globo-series glycosphingolipids displayed by Pseudomonas aeruginosa Lectin I. *J. Mol. Biol. 383*, 837−853.
(41) Beaucage, S. L., and Caruthers, M. H. (1981) Deoxynucleoside phosphoramidites - a new class of key intermediates for deoxypolynucleotide synthesis. *Tetrahedron Lett. 22*, 1859−1862.
(42) Rostovtsev, V. V., Green, L. G., Fokin, V. V., and Sharpless, K. B. (2002) A stepwise Huisgen cycloaddition process: copper(I)-catalyzed regioselective ″ligation″ of azides and terminal alkynes. *Angew. Chem., Int. Ed. 41*, 2596−2599.
(43) Tornoe, C. W., Christensen, C., and Meldal, M. (2002) Peptidotriazoles on solid phase: [1,2,3]-triazoles by regiospecific copper(I)-catalyzed 1,3-dipolar cycloadditions of terminal alkynes to azides. *J. Org. Chem. 67*, 3057−3064.
(44) Chevolot, Y., Zhang, J., Meyer, A., Goudot, A., Rouanet, S., Vidal, S., Pourceau, G., Cloarec, J. P., Praly, J. P., Souteyrand, E., Vasseur, J. J., and Morvan, F. (2011) Multiplexed binding determination of seven glycoconjugates for Pseudomonas aeruginosa Lectin I (PA-IL) using a DNA-based carbohydrate microarray. *Chem. Commun. 47*, 8826−8828.
(45) Kadam, R. U., Bergmann, M., Hurley, M., Garg, D., Cacciarini, M., Swiderska, M. A., Nativi, C., Sattler, M., Smyth, A. R., Williams, P., Camara, M., Stocker, A., Darbre, T., and Reymond, J. L. (2011) A glycopeptide dendrimer inhibitor of the galactose-specific Lectin LecA and of Pseudomonas aeruginosa biofilms. *Angew. Chem., Int. Ed. 50*, 10631−10635.
(46) Kadam, R. U., Garg, D., Schwartz, J., Visini, R., Sattler, M., Stocker, A., Darbre, T., and Reymond, J. L. (2013) CH−π "T-Shape" Interaction with histidine explains binding of aromatic galactosides to Pseudomonas aeruginosa lectin LecA. *ACS Chem. Biol. 8*, 1925−1930.
(47) Jiang, X. H., Abgottspon, D., Kleeb, S., Rabbani, S., Scharenberg, M., Wittwer, M., Haug, M., Schwardt, O., and Ernst, B. (2012) Antiadhesion therapy for urinary tract infections-a balanced PK/PD profile proved to be key for success. *J. Med. Chem. 55*, 4700−4713.
(48) Durka, M., Buffet, K., Iehl, J., Holler, M., Nierengarten, J. F., Taganna, J., Bouckaert, J., and Vincent, S. P. (2011) The functional valency of dodecamannosylated fullerenes with Escherichia coli FimH-towards novel bacterial antiadhesives. *Chem. Commun. 47*, 1321−1323.
(49) Hartmann, M., and Lindhorst, T. K. (2011) The bacterial lectin FimH, a target for drug discovery - carbohydrate inhibitors of type 1 fimbriae-mediated bacterial adhesion. *Eur. J. Org. Chem.*, 3583−3609.
(50) Touaibia, M., Wellens, A., Shiao, T. C., Wang, Q., Sirois, S., Bouckaert, J., and Roy, R. (2007) Mannosylated G(0) dendrimers with nanomolar affinities to Escherichia coli FimH. *ChemMedChem 2*, 1190−1201.
(51) Moni, L., Pourceau, G., Zhang, J., Meyer, A., Vidal, S., Souteyrand, E., Dondoni, A., Morvan, F., Chevolot, Y., Vasseur, J. J., and Marra, A. (2009) Design of triazole-tethered glycoclusters exhibiting three different spatial arrangements and comparative study of their affinities towards PA-IL and RCA 120 by using a DNA-based glycoarray. *ChemBioChem 10*, 1369−1378.
(52) Zhang, J., Pourceau, G., Meyer, A., Vidal, S., Praly, J.-P., Souteyrand, E., Vasseur, J.-J., Morvan, F., and Chevolot, Y. (2009) DNA-directed immobilisation of glycomimetics for glycoarrays application: Comparison with covalent immobilisation, and development of an on-chip IC50 measurement assay. *Biosens. Bioelectron. 24*, 2515−2521.
(53) Gillaizeau, I., Lagoja, I. M., Nolan, S. P., Aucagne, V., Rozenski, J., Herdewijn, P., and Agrofoglio, L. A. (2003) Straightforward synthesis of labeled and unlabeled pyrimidine d4Ns via 2′,3′-diyne seco analogues through olefin metathesis reactions. *Eur. J. Org. Chem.*, 666−671.